



Synthesis of Grafted Phosphorylcholine Polymer Layers as Specific Recognition Ligands for C-Reactive Protein Focused on Grafting Density and Thickness to Achieve Highly Sensitive Detection

Journal:	<i>Physical Chemistry Chemical Physics</i>
Manuscript ID:	CP-ART-01-2015-000469.R1
Article Type:	Paper
Date Submitted by the Author:	28-Feb-2015
Complete List of Authors:	Kamon, Yuri; Kobe University, Graduate School of Engineering Kitayama, Yukiya; Kobe University, Graduate School of Engineering Itakura, Akiko; National Institute for Materials Science, Fukazawa, Kyoko; The University of Tokyo, Department of Materials Engineering Ishihara, Kazuhiko; The University of Tokyo, Department of Materials Engineering Takeuchi, Toshifumi; Kobe University, Graduate School of Engineering

Synthesis of Grafted Phosphorylcholine Polymer Layers as Specific Recognition Ligands for C-Reactive Protein Focused on Grafting Density and Thickness to Achieve Highly Sensitive Detection

Yuri Kamon¹, Yukiya Kitayama¹, Akiko N. Itakura², Kyoko Fukazawa³, Kazuhiko Ishihara³,
and Toshifumi Takeuchi^{1*}

¹ Graduate School of Engineering, Kobe University, 1-1 Rokkodai-cho, Nada-ku, Kobe
657-8501, Japan

² National Institute for Materials Science, 1-2-1 Sengen, Tsukuba, Ibaraki 305-0047, Japan

³ Department of Materials Engineering, School of Engineering, The University of Tokyo,
7-3-1 Hongo, Bunkyo-ku, Tokyo 113-8654, Japan

TEL/FAX: +81-78-803-6158, E-mail: takeuchi@gold.kobe-u.ac.jp

KEYWORDS: Protein sensing, Surface-initiated activators generated by electron transfer for atom transfer radical polymerization, C-reactive protein, 2-methacryloyloxyethyl phosphorylcholine

1. Abstract

We studied the effects of layer thickness and grafting density of poly(2-methacryloyloxyethyl phosphorylcholine) (PMPC) thin layers as specific ligands for the highly sensitive binding of C-reactive protein (CRP). PMPC layer thickness was controlled by surface-initiated activators generated by electron transfer for atom transfer radical polymerization (AGET ATRP). PMPC grafting density was controlled by utilizing mixed self-assembled monolayers with different incorporation ratios of the bis[2-(2-bromoisobutyryloxy)undecyl] disulfide ATRP initiator, as modulated by altering the feed molar ratio with (11-mercaptoundecyl)tetra(ethylene glycol). X-ray photoelectron spectroscopy and ellipsometry measurements were used to characterize the modified surfaces. PMPC grafting densities were estimated from polymer thickness and the molecular weight obtained from sacrificial initiator during surface-initiated AGET ATRP. The effects of thickness and grafting density of the obtained PMPC layers on CRP

binding performance were investigated using surface plasmon resonance employing a 10 mM Tris-HCl running buffer containing 140 mM NaCl and 2 mM CaCl₂ (pH 7.4). Furthermore, the non-specific binding properties of the obtained layers were investigated using human serum albumin (HSA) as a reference protein. The PMPC layer which has 4.6 nm of thickness and 1.27 chains/nm² of grafting density showed highly sensitive CRP detection (limit of detection: 4.4 ng/mL) with low non-specific HSA adsorption, which was improved 10 times than our previous report of 50 ng/mL.

2. Introduction

Proteins play important roles in vital functions and are involved in various disease pathogenesises. Protein recognition materials with highly sensitive and selective detection abilities are therefore expected to help reveal these pathogenesises and assist in clinical diagnosis.

The C-reactive protein (CRP) is well-known as a biomarker for inflammatory diseases and organ damage, suddenly increasing in concentration in the blood when these issues develop.¹⁻⁷ Conventionally, CRP detection in clinical diagnosis is carried out by immune nephelometry and latex agglutination.^{8,9} However, these methods are limited to a

threshold of 0.3 $\mu\text{g/mL}$. Recently, highly sensitive CRP detection for concentrations below 0.15 $\mu\text{g/mL}$ has been developed for the early diagnosis of cardiovascular disease, cancer prediction, and inflammation in infants, who usually show much lower CRP levels than adults.¹⁰⁻¹³ In addition, we have reported highly sensitive CRP detection with an anti-CRP immobilized substrate utilizing surface plasmon resonance (SPR) and reflectometric interference spectroscopy, with a limit of detection (LOD) of 50 ng/mL having been achieved.¹⁴⁻¹⁶ Although using antibody recognition elements enables highly sensitive and selective detection of target proteins, the production and purification of the antibodies are complex and expensive. In addition, antibodies readily denature due to inherent instability. Therefore, alternative artificial materials that can be easily and inexpensively manufactured would be advantageous for clinical CRP detection.

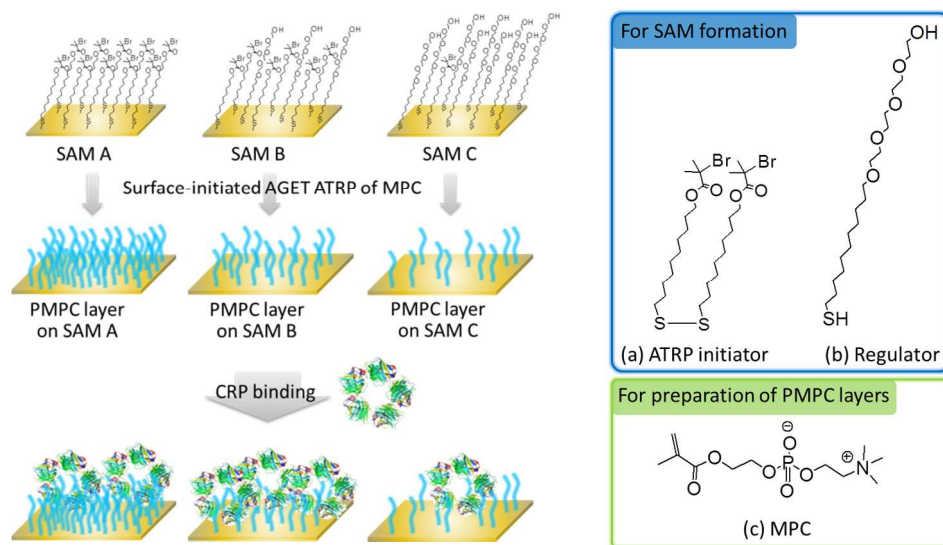
Specific ligands for target proteins are attractive alternative recognition elements because they are usually easy and inexpensive to produce and have the potential to bind to a well-defined pocket inside the target protein. The phosphorylcholine (PC) moiety in particular is known to accomplish specific binding via calcium ion coordination to CRP; the dissociation constant (K_D) of this binding is 6×10^{-5} M.¹⁷⁻²² Poly(2-methacryloyloxyethyl phosphorylcholine) (PMPC), which was originally developed by

Ishihara and coworkers, has proven particularly popular; in fact, it has been determined that materials such as nanoparticles and layers can detect CRP with a sensitivity comparable to antibodies.²³⁻²⁷ This activity results from the fact that PMPC shows not only specific interaction toward CRP but also low non-specific adsorption to other proteins present in blood due to the high hydrophilicity of the surface. In our previous work, we successfully synthesized gold nanoparticles coated in PMPC, which could detect CRP at LODs of about 50 ng/mL by using localized SPR (LSPR).²⁷

The most important factor in attaining high sensitivity with this system is the accessibility of CRP toward the specific PC moieties; because the PC groups exist on the side chains of the polymer, the polymer grafting density is of particular importance. PMPC thickness also plays an important role, because the signaling ability of both SPR and LSPR decreases exponentially as CRP binding occurs farther and farther from the gold surface. However, there are no previous reports on the effects of PMPC density and thickness with respect to CRP binding behavior.

Therefore, in this study, we investigated these effects by using PMPC thin layers with different thicknesses and grafting densities. The layers were fabricated by surface-initiated activators generated by electron transfer for atom transfer radical

polymerization (AGET ATRP)²⁷⁻³⁶, where the properties were modulated by changing polymerization time and initiator density at the surface (scheme 1). A mixed self-assembled monolayer (SAM) was employed, using varying amounts of bis[2-(2-bromoisobutyryloxy)undecyl] disulfide and (11-mercaptoundecyl)tetra(ethylene glycol) as the ATRP initiator and regulator of the initiator density on the gold substrates, respectively. Grafting density was investigated by polymers obtained from water-soluble sacrificial initiator during surface-initiated AGET ATRP.³⁷ Characterization of thickness and roughness of each SAM and PMPC thin layer was carried out by ellipsometry measurements. CRP binding behavior was investigated by SPR using a 10 mM Tris-HCl buffer containing 140 mM NaCl and 2 mM CaCl₂. Non-specific protein binding properties were also investigated with SPR using human serum albumin (HSA) as a reference protein. Overall, we attempted to demonstrate that the highly sensitive CRP detection by SPR through determination of the LOD with various PMPC substrates having different grafting density and thickness. This research will help to construct protein-sensing synthetic materials with higher sensitivity.



Scheme 1. Fabrication and CRP binding behavior of various PMPC thin layers with distinct surface polymer density by surface-initiated AGET ATRP. The chemical structures of ATRP initiator disulfide molecule (a), regulator thiol molecule (c), and MPC (c) were described.

3. Experimental Section

3-1. Preparation of self-assembled monolayer (SAM)

Typical procedure is follows. Gold-coated SPR sensor chips and gold substrate for XPS and ellipsometry measurements were rinsed with ethanol and distilled water, then cleaned by UV-O₃ treatment (20 min). The cleaned substrates were immediately immersed in an ethanol solution of 1 mM (total concentration) consisting of

bis[2-(2-bromoisobutyryloxy)undecyl] disulfide: (11-mercaptoundecyl)tetra(ethylene glycol) = 1: 0, 1: 1, 1: 20 (mol%) for 24 h at 30 °C. Afterwards, the SAM formed gold substrates were thoroughly washed with ethanol and distilled water, dried in a stream of nitrogen, and stored under vacuum pressure and light interception.

3-2. Preparation of PMPC thin layers by surface-initiated AGET ATRP

Typical procedure of preparation of PMPC thin layers by SI-AGET ATRP is follows. MPC (50 mM), CuBr₂ (1 mM), and Me₆TREN (1 mM) were dissolved in water. Each SAM-formed SPR sensor chips were fixed in a Teflon cell and submerged in this pre-polymer solution so that only one surface of the sensor chip was exposed to the solution. SAMs-formed gold substrates for XPS and ellipsometry measurements were also submerged in the solution without any fix. They were then thoroughly purged by vacuum pressure then flushed with nitrogen gas for more than 10 min. Another aqueous solution containing of ascorbic acid was added via syringe to this solution (final concentration was 0.5 mM). The solution was degassed additionally, and polymerization was induced in a water bath at 40 °C. Polymerization was stopped by exposing to air, and then the substrates were washed with pure water and submerged in 1 M EDTA-4Na aqueous solution for 24 h to remove Cu (II) ions remaining in the polymeric thin layers. After that,

obtained PMPC substrates were washed with distilled water and stored in the distilled water at 4 °C before all measurements.

3-3. SPR measurement

Binding experiments for each polymeric layer were performed at 25°C. CRP (0-100 ng/mL) and HSA (0-100 ng/mL and 1 mg/mL) each dissolved in 10 mM Tris-HCl buffer pH 7.4 containing 140 mM NaCl and 2 mM CaCl₂, were used for these experiments. Flow rate was 20 µL/min and injection volume was 20 µL. Regeneration solutions were selected appropriately from several candidates (supporting information). The amounts of bound protein were calculated from the signal intensity (resonance units, RU) at 150 sec. after protein injection finished, when the RU value reached an asymptotic steady value. All binding experiments were repeated three times. Binding isotherms were drawn using Δ RU values for each protein concentration.

4. Results and Discussion

4-1. SAM formation on gold substrate

Changing the ratio of the ATRP initiator bis[2-(2-bromoisobutyryloxy)undecyl] disulfide to the initiator density regulator (11-mercaptoundecyl)tetra(ethylene glycol) on

gold substrates allows us to prepare PMPC thin layers with various polymer densities. We have prepared three kinds of SAMs bearing different ATRP initiator densities by immersing the gold substrates in an ethanol solution of the aforementioned chemicals in order to investigate the effect of PMPC grafting density on CRP binding; feed molar ratios of 1: 0 (SAM A), 1: 1 (SAM B), and 1: 20 (SAM C), respectively, were used. Each sample was characterized by XPS and ellipsometry measurements.

Figure 1 shows the XPS spectra of the S $2p$ (a), Br $3d$ (b), C $1s$ (c), and O $1s$ (d) levels before and after immersion. The S $2p$ peak, which was not observed in the bare substrate, appeared clearly in all SAMs (Figure 1a). The peak apex was observed at around 162 eV, indicating that the S group had chemically bonded to the gold substrate. Moreover, as shown in Figure 1b, the Br $3d$ peak centered at around 68 eV was observed more clearly after immersion for SAM A; note that this peak was not clearly observed for SAMs B or C because the intensity of the Au $5p$ satellite peak centered at 74 eV overwhelmed it. However, SAMs B and C do not only show C-C (centered at around 285 eV) and C=O (centered at around 288 eV) peaks derived from the undecyl and ATRP initiator groups, but also demonstrate a notable C-O peak centered at around 286.5 eV due to the presence of the tetra ethylene glycol (TEG) groups of the regulator; this peak is much

clearer for these samples than it is for SAM A (Figure S1a). Likewise, the O 1s spectra also showed the presence of a C-O peak (centered at around 533.5 eV); again, SAMs B and C showed this more clearly than SAM A (Figure S1b).

Table S1 shows the peak area ratios of the C-C, C-O, and C=O bond elements for SAMs A, B and C, as calculated by MultiPak software. The area ratio of the C-O bonds derived from the TEG groups increased from 17.9% for SAM A to 41.2% for SAM B and 45.5% for SAM C, and the area ratio of the C=O bonds derived from the ATRP initiator tends to decrease from 9.0% for SAM A and 9.1 % for SAM B to 6.7 % for SAM C, suggesting the increase in regulator incorporation and the decrease in ATRP initiator, respectively, however, these are not accurately corresponding to initial ratio. It is because that the formation process of mixed SAM with disulfide molecules is a dynamic equilibrium that favors formation of the most energetically stable SAM regardless the feed molar ratio of disulfide molecules to thiol molecules.³⁸⁻⁴⁰ In general, molecules with hydrophobic head group such as ATRP initiator tend to assemble preferentially for molecules with hydrophilic head group such as TEG group.⁴¹ Therefore, C-O bonds derived from the TEG groups did not increase significantly and C=O bonds derived from the initiator groups did not decrease significantly even in the case of 1:20 incorporation

ratio.

Furthermore, we carried out ellipsometry experiments for all SAM-modified gold substrates, and investigated optical thickness and roughness. Each SAM thickness was calculated to be 1.0 ± 1 nm for SAM A, 2.1 ± 0.4 nm for SAM B, and 1.9 ± 0.6 nm for SAM C by fitting analysis using assuming refractive index $n = 1.5$ for each SAM. Although the relatively large deviation seems to be caused by the periodic measurements of ellipsometer due to a lot of measurements points (75 points) and large measurement area of $2 \text{ mm} \times 2 \text{ mm}$, these values are in agreement with previous reports, again suggesting successful formation.^{36, 42, 43} Here, ψ - Δ simulation curve as shown in Figure S3 describes the shifts of both ψ and Δ with increase in layer thickness on the gold substrate, whose refractive index is assumed as 1.5. Figure S3 shows Δ value decreases linearly with increase in layer thickness below 50 nm although ψ value do not significantly change, meaning that the variation of Δ values in Δ value mapping graph (25 points in 2×2 mm mapping area, as shown in Figure S4) is considered as linear change of layer thickness and available for the investigation of layer roughness. We prepared PMPC layers on all SAMs thrice by same procedures, and measured Δ values for all samples. No significant variation was observed for the bare gold substrate, indicating a flat surface, while SAM

surface roughness was more pronounced (Figure S4). These results indicate that SAM-modified gold substrates were successfully prepared.

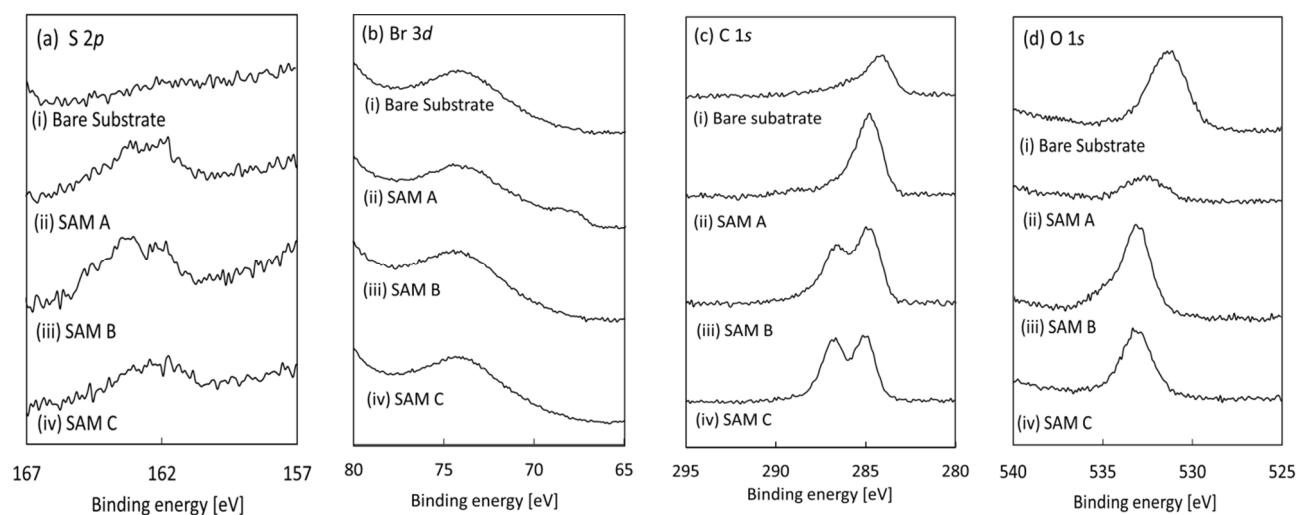


Figure 1. XPS spectra of S $2p$ (a), Br $3d$ (b), C $1s$ (c) and O $1s$ (d) before (i) and after immersing in each ethanol solution containing the thiols mixture (ii) SAM A, (iii) SAM B, and (iv) SAM C.

4-2. Surface-initiated AGET ATRP for preparation of PMPC thin layers

We prepared PMPC thin layers with different thicknesses and grafting densities by reacting the SAM bromine groups through surface-initiated AGET ATRP in water at 40 °C. We first characterized the PMPC layer grafted from SAM A by XPS and ellipsometry measurements. The N $1s$ and P $2p$ peaks, which were not observed before polymerization, appeared clearly afterward for all polymerization times (Figure 2a,b). The peak maximum

in the N 1s spectrum was observed at around 401 eV, corresponding to quaternary amine groups; this indicates successful PMPC layer formation by surface-initiated AGET ATRP. In addition, both peak area ratios N 1s/Au 4f and P 2p/Au 4f were larger after 3 h than 1 h of polymerization (Figure 3a), suggesting an increased number of MPC units over time. Ellipsometry studies yielded dried PMPC layer thicknesses of 3.4 and 4.6 nm for 1h and 3h polymerization on SAM A , respectively, based on a fitting analysis assuming $n = 1.5$ (Figure S5a); these results suggest thickness increase with polymerization time.

Next, we investigated the properties of the PMPC thin layers prepared from SAMs B and C. XPS data suggested successful grafting from SAM B given the clearly observed N 1s and P 2p peaks derived from the PC groups after polymerization as shown in Figure S2a,b. On the other hand, PMPC thin layers on SAM C have slightly P 2p peak although N 1s peak was tiny because of the inherent weak intensity of N 1s peak as shown in Figure S2 a, b, and c, suggesting the successful grafting PMPC layer on SAM C. In addition, as shown in Figure 3b, both peak area ratios N 1s/Au 4f and P 2p/Au 4f increased with increasing of the ATRP initiator incorporation ratio, suggesting an increased number of PMPC chains per unit area.

Ellipsometry studies yielded the thickness and surface roughness of dried PMPC

layers. The dried thicknesses of PMPC layers obtained for 3h polymerization on SAM A, B, and C were calculated to be $4.6 \text{ nm} \pm 0.5$, $2.1 \text{ nm} \pm 0.3$, and $1.9 \text{ nm} \pm 0.9$, respectively as shown in Figure S5b. The thicknesses of PMPC on SAM B and SAM C seem to be not significant increase compared to each SAM thickness, although XPS data supported the successful polymerization on each SAM. It is likely that the polymer chains in these samples are not perpendicular but rather laying on the substrate surface. The standard deviation of PMPC on SAM A and B in the measurement was less than 0.5 nm as shown in Figure S5b, indicating the synthesis reproducibility was good. In the case of PMPC on SAM C, the standard deviation was slightly larger (0.9 nm) than those on SAM A and B, but the value was not large. Therefore, the reproducibility of these PMPC layers was confirmed in this study. Moreover, the Δ mapping data shown in Figure S6 show differences in surface roughness due to variable incorporation of the ATRP initiator, and suggest that the PMPC layer on SAM C had the roughest surface. In addition, the surface roughness of PMPC layer on SAM C was larger compared to SAM C as shown in Figure S4d, S6c, suggesting that PMPC layer was again presumed successful grafting from SAM C.

In order to estimate the grafting densities directly, we measured the molecular

weight of PMPC chains produced from additional free sacrificial water-soluble initiators to reacting solution during polymerization for 3h, and then the grafting densities were calculated according to previous works.³⁷ (see Supporting Information) It is widely recognized that the molecular weight of free polymer chains produced from free initiator in the solution is well accordance to that of grafted polymer chains during surface-initiated ATRP.^{37, 44} As shown in Table S2, we successfully prepared monodisperse PMPC whose number average molecular weights (M_n) were calculated to be 2581 ($M_w/M_n = 1.10$) for 3h PMPC on SAM A, 2644 ($M_w/M_n = 1.12$) for 3h PMPC on SAM B, and 2688 ($M_w/M_n = 1.13$) for 3h PMPC on SAM C. The grafting densities of PMPC layers prepared on SAM A, B, and C were calculated to be 1.27, 0.56 and 0.48 chains/nm², respectively. These results suggested that the PMPC layer prepared on SAM A was concentrated polymer brush, whereas that on SAM B and C seems to be sparse brush. In surface-initiated ATRP, the densities of introduced initiators on SAM A, B, and C were related to the grafted polymer densities estimated to be 1.27, 0.56, and 0.48 chains/nm², respectively, suggesting the number of ATRP initiator on SAM A was larger than that of SAM B and C. These results further confirm the successful synthesis of PMPC thin layers different in grafting density, surface roughness, and thickness by modulating of the ratio of installed ATRP initiator.

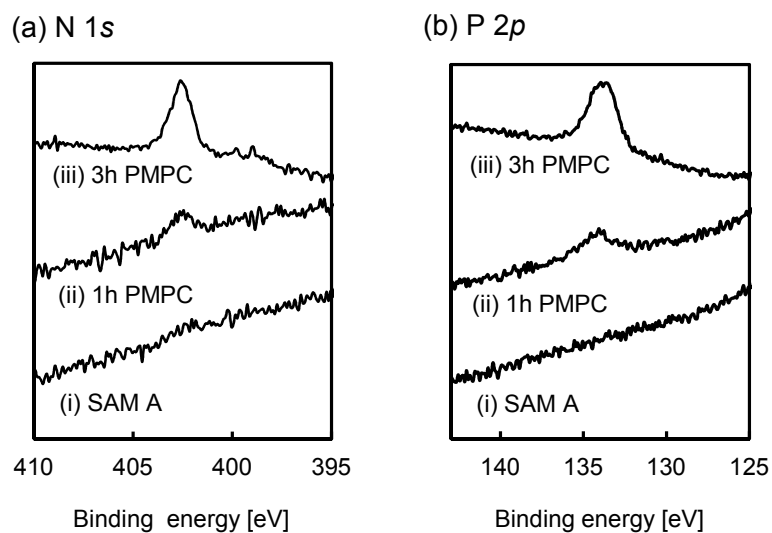


Figure 2. XPS spectra of N 1s (a) and P 2p (b) of PMPC layers obtained at 1 and 3 h polymerization on SAM A.

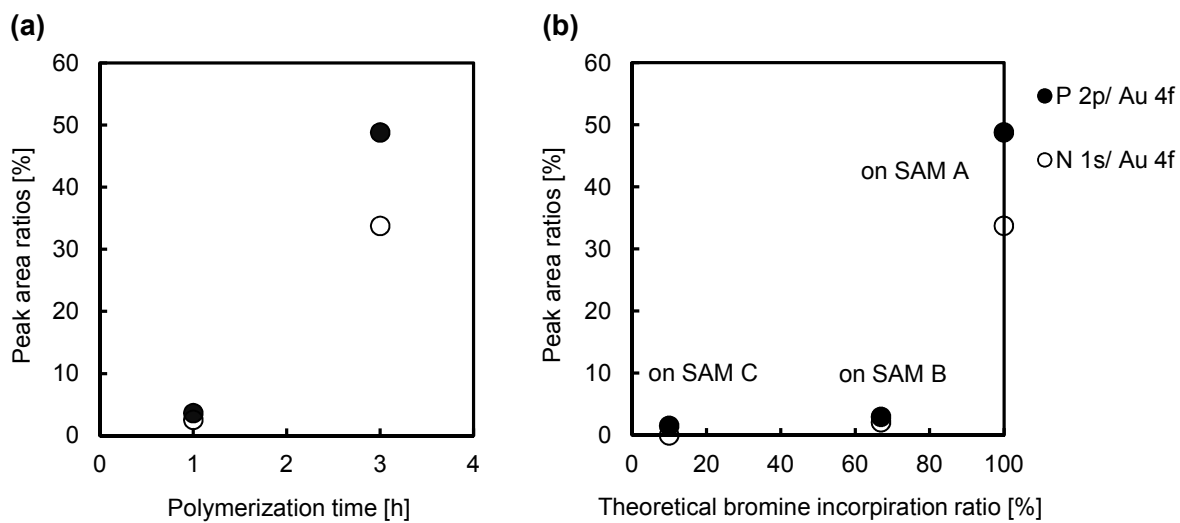


Figure 3. Comparison of the both peak area ratios (N 1s/Au 4f) and (P 2p/Au 4f) of PMPC layers obtained at 1 and 3 h polymerization time on SAM A (a) and obtained at 3h polymerization time on SAMs A, B, and C (b) derived from XPS measurements.

4-3. Comparison of CRP binding behavior in two different PMPC thicknesses

SPR measurements were used to evaluate the binding activity of CRP to the PMPC thin layers and to compare the CRP binding behavior in two different thicknesses with nanometer order such as 3.4 and 4.6 nm. CRP concentrations of 0, 5, 10, 20, 40, 80, and 100 ng/mL were tested at 25 °C using a 10 mM Tris-HCl running buffer (pH 7.4) containing 140 mM NaCl and 2 mM CaCl₂. Binding at each CRP concentration was measured 150 sec after injection, at which point RU signal was saturated. Figure 4 shows that both of PMPC layers have CRP binding ability, and the thinner dried PMPC layers with 3.4 nm showed larger Δ RU signals for all CRP injection concentrations compared to PMPC layer with 4.6 nm. In general, grafted polymer densities were essentially same in all polymerization time when the same density of installed initiator on the surface due to grafting from polymerization mechanism, and then the both PMPC layers on SAM A were relatively concentrated polymer brush calculated to be 1.27 chains/nm².⁴⁵ Moreover, the

modification of concentrated polymer brush by surface-initiated ATRP generally resulted in the depression of non-specific binding of proteins.⁴⁶ Therefore, we do not consider no significant non-specific binding happened, and it is likely that the thinness of PMPC layer enhanced the CRP binding sensitivity due to surface plasmon resonance mechanism. However, the binding behavior was not proportional to CRP concentrations and reproducibility was low. One possible reason is that slightly non-specific binding of CRP via hydrophobic interaction with SAM layer occurred due to thinness of the PMPC layer.

On the other hand, those layers obtained after 3 h of polymerization with 4.6 nm of thickness showed the most accurate CRP detection as CRP concentrations increased, with an LOD of around 4.4 ng/mL which was calculated by 3σ (σ is standard deviation of RU signal at 5 ng/mL of CRP injection concentration.). The sensitivity of this system is therefore ten times larger than our previous report of 50 ng/mL.¹⁴⁻¹⁶ These results suggested that the thickness difference affected the CRP binding behavior via SPR measurement, and in this study, PMPC layer with 4.6 nm of thickness showed the sensitive and accurate detection for CRP.

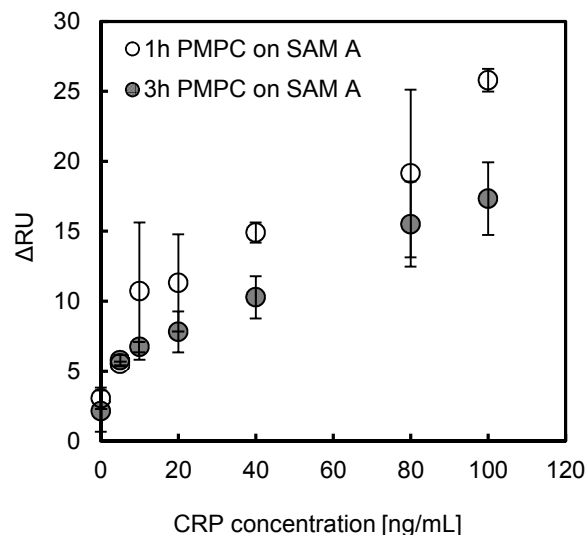


Figure 4. Binding isotherms of CRP towards PMPC thin layers obtained at 1 and 3 h polymerization on SAM A derived from SPR measurements for investigation of the dependency of CRP binding behavior on PMPC thin layer thickness.

4-4. Dependency of CRP binding behavior on PMPC thin layer polymer density

Three PMPC thin layers with different polymer grafting densities based on SAMs A (1.27 chains/nm²), B (0.56 chains/nm²), and C (0.48 chains/nm²) were prepared in order to investigate the effect of PMPC density on CRP binding behavior. As shown in Figure 5, Layers with 0.56 chains/nm² prepared from SAM B showed larger binding signals than those based on SAM A with 1.27 chains/nm², which likely results from the increased PC group accessibility in the side chains. It is attributed to be rougher surface and sparser

density of PMPC layer prepared on SAM B than that on SAM A, leading to production of voids between polymer main chains and improvement of accessibility.⁴⁷ However, the binding error was again fairly large, resulting that we cannot estimate LOD value in this detective concentration. On the other hand, ΔRU of CRP toward the PMPC layer obtained after 3 h of polymerization on SAM C was the lowest because it had a lower number of PMPC chains, meaning that the number of CRP binding sites decreased. As such, PMPC grafting density is also an important factor in CRP sensing, suggesting the potential to improve detective sensitivity by optimization of grafting density. From point of LOD, the PMPC layer on SAM A shows most sensitive detection of CRP.

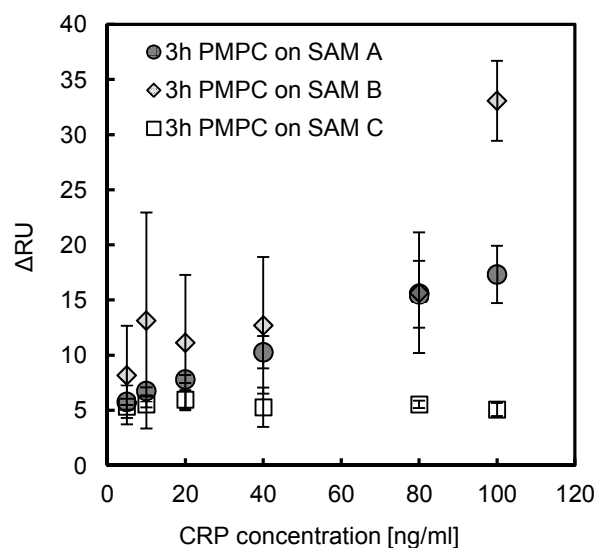


Figure 5. Binding isotherms of CRP towards PMPC thin layers based on SAMs A, B, and C for investigation of the dependency of CRP binding behavior on PMPC thin layer grafting

density.

4-5. Effects of HSA non-specific binding on polymer density and thickness

It is very important to reduce non-specific binding toward PMPC sensors in order to achieve specific detection in real samples, such as blood serum. We selected HSA as a reference protein because it accounts for 60% of serum protein and might accidentally adsorb on some polymer layers, leading to low CRP detection sensitivity.

First, we investigated non-specific adsorption at an HSA concentration below 100 ng/mL for PMPC layer obtained after 3 h of polymerization on SAM A; recall that these showed the highest LOD. Overall, no non-specific binding was observed (Figure S7), suggesting the PMPC layer has a possibility to specifically detect CRP. Next, we investigated the effects of graft density and thickness by testing all PMPC layers at HSA concentrations of 1 mg/mL. As shown in Figure 6 (a), binding of HSA on PMPC that had been polymerized for 3 h from the surfaces of SAMs B and C was 7.6 and 15 times larger than that for the corresponding SAM A sample, respectively. This difference is likely the result of variable grafting density and surface roughness - protein binding is generally greater as PMPC chain concentration decreases, as this leads to rougher and more

hydrophobic surfaces.^{48, 49} In this way, high PMPC density prevents non-specific binding while still allowing for binding of the target protein.

On the other hand, there was no significant difference in HSA binding in two thicknesses for HSA concentrations of 1 mg/mL, as the PMPC layers that had been polymerized for both 1 and 3 h on SAM A gave relatively concentrated brush. These results suggest that HSA non-specific binding is mainly affected by PMPC grafting density and surface roughness with concentrated surfaces being preferred.

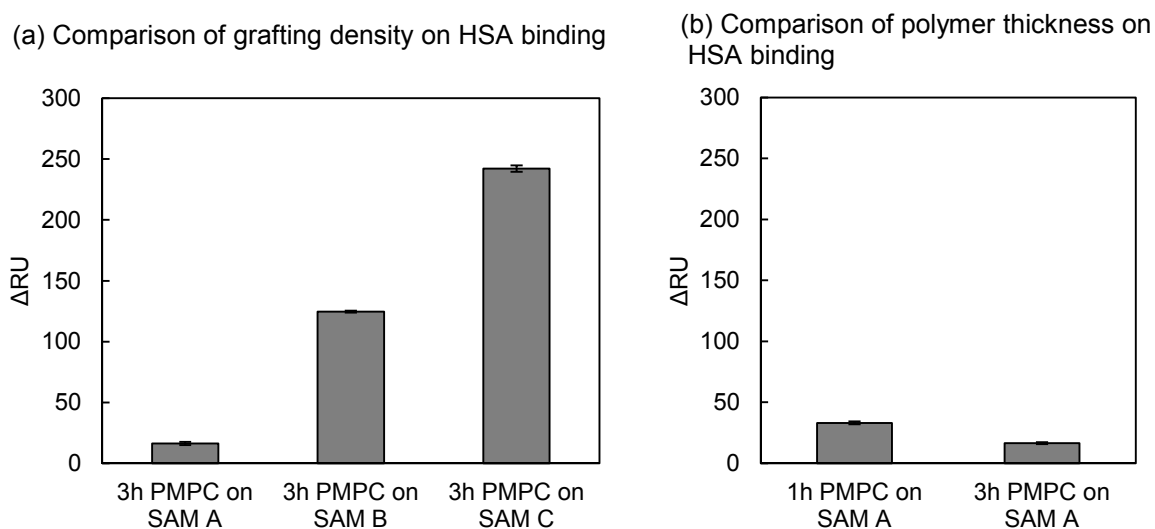


Figure 6. The Comparison of grafting density (a) and thickness (b) on HSA non-specific binding at 1 mg/mL towards PMPC thin layers.

5. Conclusions

We developed highly sensitive CRP nanosensors utilizing SPR of PMPC thin layers grafted from gold substrate, whose phosphorylcholine side chains works as specific ligands to detect CRP. To obtain PMPC thin layers with different polymer grafting density, we prepared three kinds of SAMs with different incorporation ratios of the bis[2-(2-bromoisobutyryloxy)undecyl] disulfide ATRP initiator by modulating the feed ratio of the compound with an (11-mercaptopundecyl)tetra(ethylene glycol) regulator in ethanol solution. The PMPC layers were then grown off the produced SAMs by a surface-initiated AGET ATRP lasting 1 or 3 h. XPS and ellipsometry studies revealed that the obtained layers had different chemical composition, surface roughness, and thickness from each other depending on the polymerization time and the ATRP initiator feed ratio. Moreover, the obtained PMPC layers had three different grafting densities depending on the installed ATRP initiator ratios. CRP binding properties were significantly affected by surface roughness and grafting density. While reproducibility was low, the layers with rougher surface and 0.56 chains/nm^2 of grafting density prepared on SAM B showed the largest binding of CRP by SPR, which was attributed to the greater accessibility of the PC moieties on the PMPC side chains. More importantly, we successfully achieved a high detection limit of 4.4 ng/mL for the PMPC layer grafted from SAM A; the layer had a

thickness of 4.6 nm and 1.27 chains/nm² of grafting density, which improved the sensitivity to more than 10 times compared to our previously reported value of 50 ng/mL utilizing immobilized PMPC nanomaterials. This level of sensitivity is sufficient for use in early CRP detection. Moreover, HSA non-specific binding experiments indicated that grafting density and surface roughness significantly affect non-specific binding compared to thickness. The PMPC layer on SAM A that had a thickness of 4.6 nm and 1.27 chains/nm² of grafting density showed the lowest non-specific binding.

Overall, these experiments suggest that the more detail optimization of layer thickness, PMPC grafting density, and surface roughness can together allow for high selectivity and sub-nanomolar CRP detection. We believe this work will significantly contribute to the fabrication of CRP sensors for the early clinical diagnosis of inflammation, coronary heart disease, and cancer.

References

- 1 J. P. Casas, T. Shah, A. D. Hingorani, J. Danesh and M. B. Pepys, *J. Internal Med.*, 2008, **264**, 295-314.
- 2 S.-F. Yang, T.-F. Wu, H.-T. Tsai, L.-Y. Lin and P.-H. Wang, *Clin. Chem. Acta*, 2014, **431**,

118-124.

3 M. B. Pepys and G. M. Hirschfield, *J. Clin. Invest.*, 2003, **111**, 1805-1812.

4 R. P. Tracy and L. H. Kuller, *Arch. Intern. Med.*, 2005, **165**, 2058-2060.

5 D. M. Steel and A. S. Whitehead, *Immunol. Today*, 1994, **15**, 81-88.

6 C. Sjöwall, A. A. Bengtsson, G. Sturfelt and T. Skogh, *Arthritis Res. Ther.*, 2004, **6**,
87-94.

7 L. H. Kuller, R. P. Tracy, J. Shaten and E. N. Meilahn, *Am. J. Epidemiol.* 1996, **144**,
537-547.

8 S. P. Amodio, P. Holownia, C. L. Davey and C. P. Price, *Anal. Chem.*, 2001, **73**,
3417-3425.

9 P. Holownia, S. P. Amodio and C. P. Price, *Anal. Chem.*, 2001, **73**, 3426-3431.

10 S. Kitahashi, N. Tatsumi, S. Tagawa, T. Matsui, M. Higashihata, H. Shintaku, S.
Tomoda and I. Tsuda, *J. Autom. Chem.*, 1998, **20**, 195-198.

11 B. Shine, J. Gould, C. Campbell, P. Hindocha, R. P. Wilmot and C. B. S. Wood, *Clin.*
Chim. Acta, 1985, **148**, 97-103.

12 N. Rifai and P. M. Ridker, *Clin. Chem.*, 2001, **47**, 403-411.

13 S. Bassuk, N. Rifai and P. M. Ridker, *Curr. Probl. Cardiol.*, 2004, **29**, 439-493.

- 14 H. W. Choi, Y. Sakata, Y. Kurihara, T. Ooya and T. Takeuchi, *Anal. Chim. Acta*, 2012, **728**, 64-68.
- 15 A. Murata, T. Ooya and T. Takeuchi, *Biosens. Bioelectron.*, 2013, **43**, 45-49.
- 16 A. Murata, T. Ooya and T. Takeuchi, *Microchim. Acta*, 2014, in press, DOI 10.1007/s00604-014-1334-2.
- 17 T. Christopeit, T. Gossas and U. H. Danielson, *Anal. Biochem.*, 2009, **391**, 39-44.
- 18 R. Casey, J. Newcombe, J. McFadden and K. B. Bodman-Smith, *Inf. Immun.*, 2008, **76**, 1298-1304.
- 19 S. J. Swanson, B.-F. Lin, M. C. Mullenix and R. F. Mortensen, *J. Immunol.*, 1991, **146**, 1596-1601.
- 20 C. M. Kinoshita, S.-C. Ying, T. E. Hugli, J. N. Siegel, L. A. Potempa, H. Jiang, R. A. Houghten and H. Gewurz, *Biochemistry*, 1989, **28**, 9840-9848.
- 21 J. E. Volanakis and K. W. A. Wirtz, *Nature*, 1979, **281**, 155-157.
- 22 S. A. Drieghe, H. Alsaadi, P. L. Tugirimana and J. R. Delanghe, *Clin. Chem. Lab. Med.*, 2014, **52**, 861-867.
- 23 K. Ishihara, T. Ueda and N. Nakabayashi, *Polym. J.*, 1990, **22**, 355-360.
- 24 Y. Iwasaki, T. Kimura, M. Orisaka, H. Kawasaki, T. Goda and S. Yusa, *Chem. Commun.*,

2014, **50**, 5656-5658.

25 T. Goda, P. Kijall, K. Ishihara, A. R. Dahlfors and Y. Miyahara, *Adv. Healthcare Mater.*, 2014, **3**, 1733–1738.

26 E. Kim, H. C. Kim, S. G. Lee, S. J. Lee, T. J. Go, C. S. Baek and S. W. Jeong, *Chem. Commun.*, 2011, **47**, 11900-11902.

27 Y. Kitayama and T. Takeuchi, *Anal. Chem.*, 2014, **86**, 5587-5594.

28 J. S. Wang and K. Matyjaszewski, *Macromolecules*, 1995, **28**, 7901-7910.

29 K. Matyjaszewski and J. Xia, *Chem. Rev.*, 2001, **101**, 2921-2990.

30 K. Min, H. F. Gao and K. Matyjaszewski, *J. Am. Chem. Soc.*, 2005, **127**, 3825-3830.

31 M. Kato, M. Kamigaito, M. Sawamoto and T. Higashimura, *Macromolecules*, 1995, **28**, 1721-1723.

32 D.J. Siegwart, J. K. Oh and K. Matyjaszewski, *Prog. Polym. Sci.*, 2012, **37**, 18-37.

33 S. Sasaki, Y. Kitayama, T. Ooya and T. Takeuchi, *J. Biosci. Bioeng.*, 2014, in press, DOI:10.1016/j.jbiosc.2014.06.019.

34 M. Ishio, M. Katsube, M. Ouchi, M. Sawamoto and Y. Inou, *Macromolecules*, 2009, **42**, 188-193.

35 Y. Kitayama and T. Takeuchi, *Langmuir*, 2014, **30**, 12684–12689.

- 36 Y. Kamon, R. Matsuura, Y. Kitayama, T. Ooya and T. Takeuchi, *Polym. Chem.*, 2014, **5**, 4764-4771.
- 37 K. Matyjaszewski, H. Dong, W. Jakubowski, J. Pietrasik, and A. Kusumo, *Langmuir*, 2007, **23**, 4528-4531.
- 38 J. C. Love, L. A. Estroff, J. K. Kriebel, R. G. Nuzzo, and G. M. Whitesides, *Chem. Rev.*, 2005, **105**, 1103-1169.
- 39 P. E. Laibinis, M. A. Fox, J. P. Folkers and G. M. Whitesides, *Langmuir*, 1991, **7**, 3167-3173.
- 40 Y.-S. Shon, C. Mazzitelli and R. W. Murray, *Langmuir*, 2001, **17**, 7735-7741.
- 41 C. D. Bain, J. Evall, and G. M. Whitesides, *J. Am. Chem. Soc.*, 1989, **111**, 7155–7164.
- 42 E. Rakhmatullina, T. Braun, T. T. Kaufmann, H. Spillmann, V. Malinova and W. Meier, *Macromol. Chem. Phys.*, 2007, **208**, 1283-1293.
- 43 B. S. Lee, Y. S. Chi, K.-B. Lee, Y.-G. Kim and I. S. Choi, *Biomacromolecules*, 2007, **8**, 3922-3929.
- 44 K. Ohno, Y. Kayama, V. Ladmiral, T. Fukuda, and Y. Tsujii, *Macromolecules*, 2010, **43**, 5569–5574.
- 45 W. Fenga, J. L. Brasha and S. Zhu, *Biomaterials*, 2006, **27**, 847–855.

46 Y. Inoue and K. Ishihara, *Colloids Surf., B*, 2010, **81**, 350–357.

47 S.-F. Sui, Y.-T. Sun and L.-Z. Mi, *Biophys. Jour.*, 1999, **76**, 333-341.

48 W. Feng, J. L. Brash and S. Zhu, *Biomaterials*, 2006, **27**, 847-855.

49 W. Feng, S. Zhu, K. Ishihara and J. L. Brash, *Langmuir*, 2005, **21**, 5980-5987.

TOC Graphic

